The Astrophysical Journal Letters, 821:L31 (5pp), 2016 April 20 doi:10.3847/2041-8205/821/2/L31

FIRST DETECTION IN GAMMA-RAYS OF A YOUNG RADIO GALAXY: *FERMI*-LAT OBSERVATIONS OF THE COMPACT SYMMETRIC OBJECT PKS 1718–649

G. Migliori[1], A. Siemiginowska[2], M. Sobolewska[2,3], A. Loh[1], S. Corbel[1,4], L. Ostorero[5], and Ł. Stawarz[6]

[1] Laboratoire AIM (CEA/IRFU—CNRS/INSU—Université Paris Diderot), CEA DSM/SAp, F-91191 Gif-sur-Yvette, France; giulia.migliori@cea.fr

[2] Harvard-Smithsonian Center for Astrophysics, 60 Garden Street, Cambridge, MA 02138, USA

[3] Nicolaus Copernicus Astronomical Center, Bartycka 18, 00-716 Warsaw, Poland

[4] Station de Radioastronomie de Nançay, Observatoire de Paris, CNRS/INSU, Univ. Orléans, F-18330 Nançay, France

[5] Dipartimento di Fisica, Università degli Studi di Torino and Istituto Nazionale di Fisica Nucleare (INFN), Via P. Giuria 1, I-10125 Torino, Italy

[6] Astronomical Observatory, Jagiellonian University, ul. Orla 171, 30-244 Kraków, Poland

Received 2016 March 24; revised 2016 April 5; accepted 2016 April 6; published 2016 April 20

ABSTRACT

We report the γ-ray detection of a young radio galaxy, PKS 1718−649, belonging to the class of compact symmetric objects (CSOs), with the Large Area Telescope (LAT) on board the *Fermi* satellite. The third *Fermi* Gamma-ray LAT catalog (3FGL) includes an unassociated γ-ray source, 3FGL J1728.0−6446, located close to PKS 1718−649. Using the latest Pass 8 calibration, we confirm that the best-fit 1σ position of the γ-ray source is compatible with the radio location of PKS 1718−649. Cross-matching of the γ-ray source position with the positions of blazar sources from several catalogs yields negative results. Thus, we conclude that PKS 1718−649 is the most likely counterpart to the unassociated LAT source. We obtain a detection test statistics TS $\sim$ 36 ($>5\sigma$) with a best-fit photon spectral index $\Gamma = 2.9 \pm 0.3$ and a 0.1–100 GeV photon flux density $F_{0.1-100\,\mathrm{GeV}} = (11.5 \pm 0.3) \times 10^{-9}$ ph cm^{-2} s^{-1}. We argue that the linear size ($\sim$2 pc), the kinematic age ($\sim$100 years), and the source distance ($z = 0.014$) make PKS 1718−649 an ideal candidate for γ-ray detection in the framework of the model proposing that the most compact and the youngest CSOs can efficiently produce GeV radiation via inverse-Compton scattering of the ambient photon fields by the radio lobe non-thermal electrons. Thus, our detection of the source in γ-rays establishes young radio galaxies as a distinct class of extragalactic high-energy emitters and yields a unique insight on the physical conditions in compact radio lobes interacting with the interstellar medium of the host galaxy.

Key words: galaxies: active – galaxies: individual (PKS 1718, 649) – galaxies: jets – gamma rays: galaxies – radiation mechanisms: non-thermal

1. INTRODUCTION

The radio-loud active galactic nuclei (RL AGNs) constitute nearly 60% of all the γ-ray sources detected in the first four years of the all-sky survey of the Large Area Telescope (LAT) on board the *Fermi* satellite and are listed in the Third *Fermi* Gamma-ray LAT catalog (3FGL; Acero et al. 2015). The overwhelming majority (98%) of the RL AGNs in the 3FGL have been classified as blazars, i.e., AGNs with relativistic jets oriented close to the line of sight of the observer (see the Third LAT AGN Catalog, 3LAC; Ackermann et al. 2015). The remaining 2% of the LAT AGNs includes mostly radio galaxies whose jets point away from the observer, the so-called misaligned AGNs (MAGNs; Abdo et al. 2010a), and a few AGNs of other types (see Massaro et al. 2015 for a review). About one-third of the 3FGL sources is still unidentified (1010 over 3033), and it is among them that we may expect to discover new classes of γ-ray emitters.

In blazars, Doppler-boosted γ-ray emission is produced in a compact, relativistically moving jet region close to the AGN. The origin of the emission detected by *Fermi*-LAT in MAGNs is less clear (Abdo et al. 2010a, Kataoka et al. 2011), and models of stratified jets or extended emitting regions have been considered. So far, given the point-spread function (PSF) of *Fermi*-LAT, Centaurus A remains the only radio galaxy in the 3FGL associated with a γ-ray component that clearly extends beyond the central nuclear region and contributes more than $\sim$50% of the total γ-ray flux (Abdo et al. 2010b). This extended γ-ray emission spatially coincides with the giant radio lobes of Centaurus A, and it is consistent with inverse Comptonization (IC) of the relic cosmic microwave background (CMB) radiation. In Centaurus A, the detection and imaging of the diffuse γ-ray emission, which is isotropic and not boosted by relativistic effects, is likely possible because of the source physical extension ($\sim$600 kpc) and proximity (distance of $\sim$3.6 Mpc).

Compact radio sources with radio structures fully contained within the central regions of their host galaxies ($<$1 kpc) are thought to be the progenitors of the large-scale radio galaxies (lobes' linear sizes of tens to hundreds of kiloparsecs). The initial stage of the radio source growth is represented by compact symmetric objects (CSOs) with sub-kiloparsec-scale structures, symmetric radio morphologies, total radio emission dominated by the mini-lobes, and kinematical ages smaller than a few thousand years (review by Orienti 2016). CSOs belong to the spectral class of gigahertz-peaked spectrum (GPS) radio galaxies, characterized by a stable, convex radio spectrum peaking at GHz frequencies (see O'Dea 1998 for a review). Some theoretical models predict that CSOs should be relatively strong γ-ray emitters as their compact radio lobes contain copious amount of highly relativistic particles and are embedded in an environment rich in low-energy photons (see Stawarz et al. 2008; Ostorero et al. 2010). During the initial phase of expansion, the lobes could be the sites of production of bremsstrahlung γ-ray emission potentially detectable by *Fermi*-LAT (Kino et al. 2009). The radio lobes are expanding at sub-relativistic velocities; therefore, the γ-ray emission is expected to be isotropic and steady on short timescales (up to

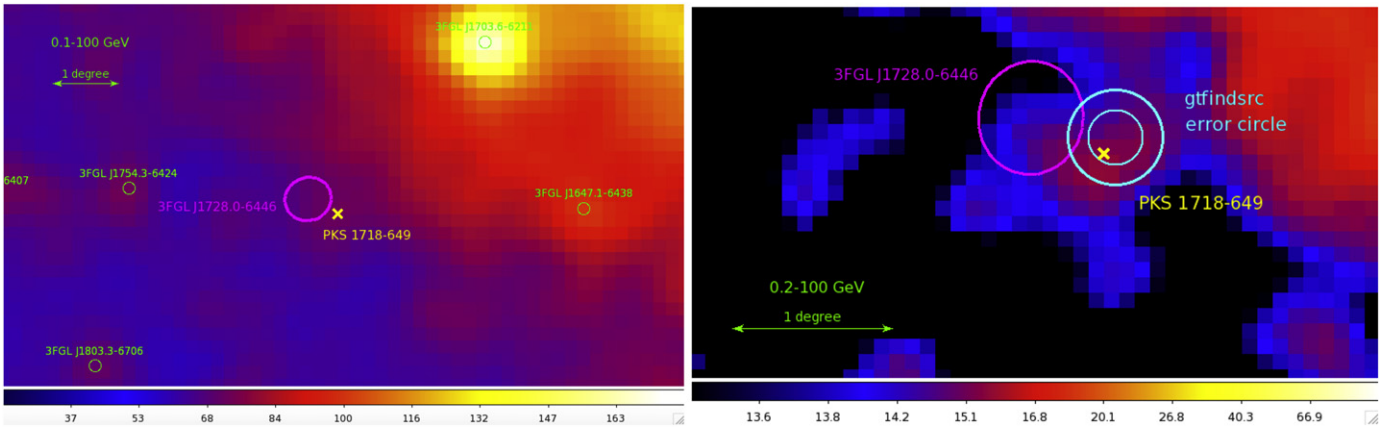

Figure 1. Left: *Fermi*-LAT 0.1–100 GeV count map of the sky centered on the radio position of PKS 1718−649 (yellow cross). The pixel size is 0.2 degrees/pixel. The magenta ellipse gives the uncertainty position (95% confidence level) of 3FGL J1728.0−6446 reported in the 3FGL. Field γ-ray sources in the 3FGL are indicated with green circles. Right: zoom on the PKS 1718−649 region at >200 MeV energies. The pixel size is 0.1 degrees/pixel. The cyan circles correspond to the *gtfindsrc* best-fit position (68% and 95% confidence levels).

months/years). However, detections of the γ-ray emission from young radio sources have been so far elusive even with *Fermi* (Migliori et al. 2014; D'Ammando et al. 2016).

In this Letter, we report for the first time the detection with *Fermi*-LAT of γ-ray emission from the nearby ($z = 0.014$) GPS radio galaxy PKS 1718−649 (Tingay et al. 2015 and references therein). The double-lobed, compact (∼2 pc) radio morphology of PKS 1718−649 and its estimated age ($t_{\rm age} \sim 100$ years; Giroletti & Polatidis 2009) make this source one of the youngest in the class of CSOs. Throughout the Letter we assume a ΛCDM cosmology with $H_0 = 70\,{\rm km\,s^{-1}\,Mpc^{-1}}$, $\Omega_M = 0.3$, and $\Omega_\Lambda = 0.7$.

2. OBSERVATIONS

PKS 1718−649 belongs to the CSO sample selected for a γ-ray study with *Fermi*-LAT (Migliori 2016). This initial analysis of five-year accumulation of the *Fermi*-LAT data resulted in a marginal detection (≈4σ) of a faint γ-ray source at the radio position of PKS 1718−649, $F_{0.1-100\,{\rm GeV}} = (1.5 \pm 0.7) \times 10^{-8}\,{\rm ph\,cm^{-2}\,s^{-1}}$. The 3FGL contains an unassociated γ-ray source (3FGL J1728.0-6446) detected at the 4.4σ level with a slightly different location, for which PKS 1718−649 lies just outside the 95% uncertainty radius (Figure 1, left panel; Table 2). We thus performed a new analysis to assess the significance, flux, and location of the γ-ray source, exploiting the improved data quality and statistics of the new Pass 8 data release.

We analyzed seven years of the *Fermi*-LAT data (observations from 2008 August 8 to 2015 August 8). We selected events of the Pass 8 (P8R2) Source class (Atwood et al. 2013) and used the adequate instrument response functions for the analysis (P8R2_V6) and the Science Tools software package version v10r0p5. The standard event selections were applied: we used FRONT and BACK events and applied a zenith angle cut at 90° to eliminate Earth limb events. We made use of both the binned and unbinned analyses. Given the long computational times due to the large data set, we limited the unbinned analysis to consistency checks and, most importantly, to secure the source localization.

We first considered the 0.2−100 GeV band to minimize the systematic errors and study the background contamination (Ackermann et al. 2012). Next, we increased the photon statistics by lowering the minimum energy threshold to 0.1 GeV. In the latter case, we excluded the data with the lowest quality of the reconstructed direction[7] (evtype = 56) and applied a zenith angle cut at 80° to minimize the contribution of the background γ-rays from the Earth's limb. We selected a circular region of interest (RoI) of 15° radius, centered on the radio position of PKS 1718−649.

The *Fermi* source model that we adopted to calculate the binned likelihood includes all the 3FGL point-like and diffuse sources within the RoI. Additionally, we included the 3FGL sources falling between 15° and 25°. In fact, due to the energy-dependent size of the *Fermi*-LAT PSF, these sources can contribute to the total counts observed within the RoI. The 3FGL only accounts for sources detected within the first four years of observations. Therefore, we carefully applied this initial model to the seven-year data set, and whenever necessary, we improved it by, e.g., adding sources that were detected in the following three years. In order to assess the fit quality, we inspected the residual maps obtained by comparing the *Fermi*-LAT count map with a count map created from the best-fit model. For example, we added a variable radio source, PKS 1824−582, located ∼10.°3 from the RoI center (flaring in April 2014; ATel #6067, ATel #6076). The photon spectral indices, Γ, of the faintest sources within 7° from the RoI center were fixed to the values reported in the 3FGL. For sources located 7° away from the RoI center, all the spectral parameters were initially fixed to the respective 3FGL values. We opportunely modified these values, whenever the inspection of the residuals revealed a significant variation of a source (e.g., 3FGL J1703.6-6211; ATel #7330).

The emission model also accounts for the Galactic and extragalactic (and instrumental) diffuse backgrounds. We used the "mapcube" file `gll_iem_v06.fits` and the `iso_P8R2_V6_v06.txt` table to describe the emission from the Milky Way and the isotropic component, respectively.

To test the hypothesis that the γ-ray source reported in the 3FGL is associated with PKS 1718−649, in the model we substituted 3FGL J1728.0-6446 with a source located at the radio position of PKS 1718−649, assuming a power-law spectrum model ($F = KE^{-\Gamma}$). We performed a fit of the data using the binned maximum likelihood (*gtlike*). The temporal

[7] http://fermi.gsfc.nasa.gov/ssc/data/analysis/documentation/Cicerone/Cicerone_Data/LAT_DP.html.

Table 1
PKS 1718−649—LAT Binned Analysis Results

Energy Band (1)	Time (2)	TS (3)	Γ (4)	*Fermi*-LAT Flux (5)	Log(νF_ν, 1 GeV) (6)
7 Year Data Set					
0.1–100	54686.49–57242.49	36	2.9 ± 0.3	11.5 ± 0.3	−12.4 ± 0.1
0.2–100	54686.49–57242.49	18.5	2.6 ± 0.3	2.1 ± 0.8	−12.4 ± 0.2
Incremental Analysis					
0.1–100	54686.49–56147.49	15	2.9(f)	9.8 ± 2.8	−12.4 ± 0.13
0.1–100	54686.49–56512.49	19	2.9(f)	9.8 ± 2.5	−12.4 ± 0.11
0.1–100	54686.49–56877.49	28	2.9(f)	10.9 ± 2.3	−12.4 ± 0.09

Note. Columns: 1—Energy band selected for the analysis in GeV; 2—Observing time in Modified Julian Day; 3—Test statistic value; 4—Gamma-ray photon spectral index, (f) indicates fixed Γ; 5—*Fermi*-LAT photon flux in the selected energy band in units of $\times 10^{-9}$ ph cm^{-2} s^{-1}; 6—Logarithm of the flux density at 1 GeV in erg cm^{-2} s^{-1}.

behavior of the source was investigated with a light curve with one-year time resolution, and in an incremental way, i.e., by progressively summing the years of observation. Quoted errors are at 1σ statistical significance, if not otherwise specified.

3. RESULTS

The results of the binned likelihood analysis performed on the seven-year data set for the two low-energy cutoffs are shown in Table 1. The binned analysis of the 0.2−100 GeV data set yielded γ-ray emission detected at the PKS 1718−649 position with a test significance[8] TS = 18.5 ($\sigma \sim 4.3$), which improves over the TS = 14 of our previous five-year-data analysis (Migliori 2016). We obtained an integrated source photon flux density above 0.2 GeV $F_{0.2-100\ \mathrm{GeV}} = (2.1 \pm 0.8) \times 10^{-9}$ ph cm^{-2} s^{-1} and a best-fit photon spectral index $\Gamma = 2.6 \pm 0.3$.

The results improved when the analysis was extended to the 0.1–100 GeV band. We obtained a TS ∼ 36 detection ($\gtrsim 5\sigma$) at the location of PKS 1718−649. The best-fit photon spectral index, $\Gamma = 2.9 \pm 0.3$, is steeper than that measured at ⩾0.2 GeV, but the two values are consistent within the uncertainties. As a check, we restricted the analysis to the two best-quality quartiles of the data in the PSF type partition (event types PSF2 and PSF3), i.e., the data with the best quality of the reconstructed direction of the photons. We used the Python package `SummedLikelihood` to combine the likelihoods of the separately analyzed (PSF2 and PSF3 type) data sets. Despite the significant cut in event number, we detected a source at the position of PKS 1718−649 with a TS ∼ 24 and spectral parameters consistent within the uncertainties with the 0.1−100 GeV best-fit values.

The source is not detected at a significance level exceeding TS = 10 on yearly timescales. The incremental time analysis shows that the source begins to be significantly detected over 4 years. The TS value progressively increases over 5, 6, and 7 years, whereas the measured flux does not vary significantly (Table 1).

[8] The test statistic is the logarithmic ratio of the likelihood of a source being at a given position in a grid to the likelihood of the model without the source, TS = 2log(likelihood$_{\mathrm{src}}$/likelihood$_{\mathrm{null}}$) (Mattox et al. 1996).

Table 2
PKS 1718−649 Gamma-Ray Best-fit Position

Source (1)	R.A. (2)	Decl. (3)	Position Uncertainty. (4)
γ-Ray Position			
3FGL J1728.0 −6446	17 28 02.29	−64 46 23.08	0.23 × 0.20[a] (P.A. = 79.°5) 0.37 × 0.32[a] (P.A. = 79.°5)
gtfindsrc best fit position	17 22 57.60	−64 54 24.48	0.18[b] 0.31[b]
Radio Position			
PKS 1718−649	17 23 41.0	−65 00 36.6	0.0020 × 0.00095[c]

Notes. Columns: 1—Source; 2 and 3—Source coordinates (R.A. in hh mm ss.d and decl. in dd mm ss.d); 4—Position uncertainty.
[a] Semimajor and semiminor axes in degrees of the ellipse uncertainty region at 68% and 95% confidence level respectively, followed by the position angle of the 95% confidence region (reported in the 3FGL).
[b] Uncertainty radius of the best-fit *gtfindsrc* position at 68% and 95% confidence level in degrees.
[c] Uncertainty on the radio position in arcseconds (Johnston et al. 1995).

3.1. Gamma-Ray Source Association

In order to optimize the localization of the γ-ray source, we ran the *gtfindsrc* tool, which calculates the best TS for different positions given an initial guess (in this case, PKS 1718−649 coordinates) until the convergence tolerance for a positional fit is reached. The best-fit position and the corresponding 68% and 95% error radii are reported in Table 2. PKS 1718−649 lies within the 68% confidence radius, at a distance of 0.°13 from the best-fit γ-ray position (Figure 1, right panel). We evaluated the significance of a γ-ray source located at the position of 3FGL J1728.0-6446 using the 0.1–100 GeV and the 0.2–100 GeV data sets, and we obtained lower TS values ($<4\sigma$) than for PKS 1718−649. Finally, we fit to the data a model with two distinct emitters located at the positions of PKS 1718−649 and 3FGL J1728.0-6446: the γ-ray emission in excess over the background is attributed to the former, whereas the latter has TS ∼ 0.

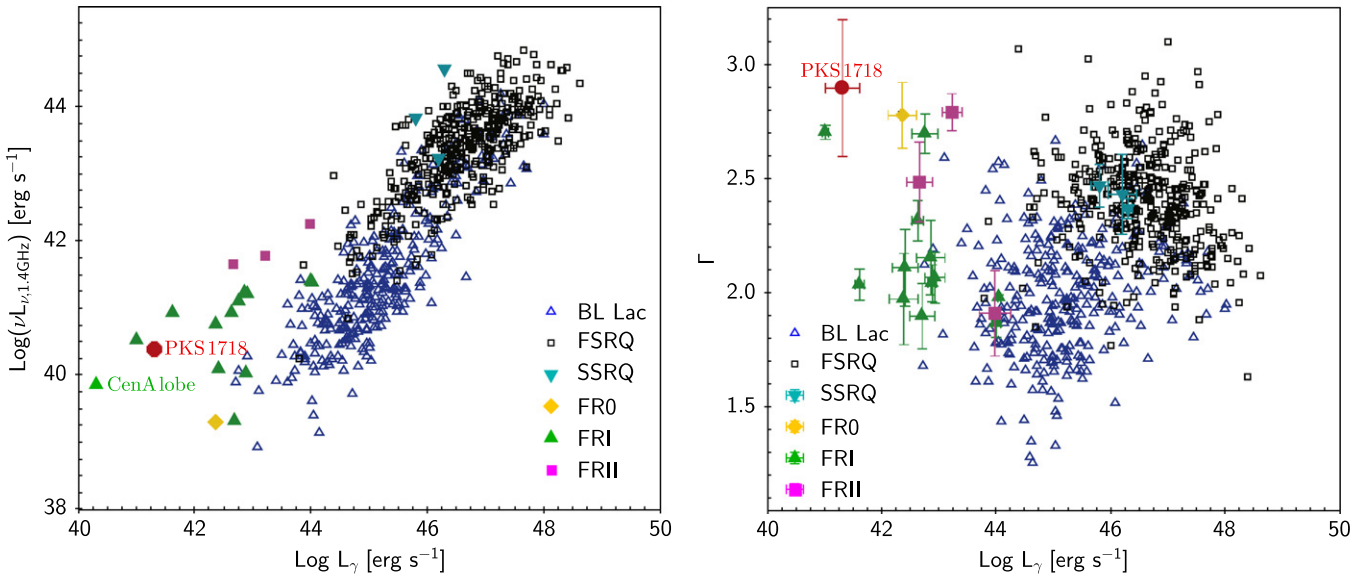

Figure 2. Left: radio luminosity of the 3LAC FR I (solid, green triangles) and FR II (solid, magenta squares) radio galaxies, BL Lacs (open, open triangles), FSRQs (open, black squares), and SSRQs (cyan, solid triangles) plotted as a function of the γ-ray luminosity between 1 and 100 GeV. We included Tol1326-379 (solid, yellow diamond), classified as FR 0 (Grandi et al. 2015), and the γ-ray detected lobes of Centaurus A (the south lobe with measured γ-ray and 1.4 GHz fluxes; see Abdo et al. 2010b and Hardcastle et al. 2009, respectively). The position of PKS 1718−649 is indicated by the solid, red circle. Right: γ-ray spectral index versus 1–100 GeV luminosity. PKS 1718−649 is located in the MAGN region of the diagram, with values of Γ and L_γ similar to those of Centaurus A. (Sample data: courtesy of P. Grandi.)

We searched for other counterparts to the detected γ-ray source in catalogs and surveys of blazars and extragalactic radio sources, including the Roma BZCAT (Massaro et al. 2009), a catalog of γ-ray candidates among *WISE* sources (D'Abrusco et al. 2014), the Combined Radio All-Sky Targeted Eight GHz Survey (CRATES; Healey et al. 2009), the Parkes Catalog (Wright & Otrupcek 1990), and the Parkes-MIT-NRAO survey (PMN; Gregory et al. 1994), and found no match within the *gtfindsrc* 95% error circle. At low radio frequencies (843 MHz), a query to the Sydney University Molonglo Sky Survey (SUMSS; Mauch et al. 2003) returned 15 radio sources within the error circle. However, PKS 1718−649 is: (1) the brightest source at 843 MHz, with a flux density $F_{843\ \mathrm{MHz}} = (3.7 \pm 0.1)$ Jy; (2) the only source reported in the high radio frequency catalogs, with a detection at 5.0 and 8.4 GHz, and a counterpart in the Two Micron All Sky Survey (2MASS; Skrutskie et al. 2006). For the remaining 14 SUMSS sources, the flux faintness (only three of them have 843 MHz fluxes in the 100–200 mJy range), non-detection at the higher frequencies, and lack of a 2MASS counterpart strongly disfavor the identification with an extragalactic, flat-spectrum radio source. We concluded that there are no evident blazar candidates in the 95% error circle of the γ-ray source.

4. DISCUSSION AND CONCLUSIONS

Our analysis of the seven-year *Fermi*-LAT data resulted in a $>5\sigma$ detection of the γ-ray source 3FGL J1728.0−6446, which had no association in the 3FGL catalog. Based on our revised best-fit γ-ray position and the analysis of nearby sources, we concluded that this source is most likely the γ-ray counterpart to PKS 1718−649, a young radio galaxy classified as CSO. This represents the first significant ($>5\sigma$) γ-ray detection of a bona fide CSO, and it may provide us with important insights on the nature of the high-energy emission observed in young radio sources.

We compared the γ-ray properties of PKS 1718−649 with those of blazars and MAGNs from the clean 3LAC sample. We considered only blazars with known redshift and classified them as either flat-spectrum radio quasars (FSRQs) or BL Lac objects. The MAGN sample includes steep-spectrum radio quasars (SSRQs), Fanaroff–Riley (FR) type I and type II radio galaxies (Fanaroff & Riley 1974) detected by *Fermi*-LAT[9], and Tol1326-379, the only FR 0 radio galaxy[10] associated with a γ-ray source (Grandi et al. 2015). Figure 2 shows the position occupied by PKS 1718−649 in the radio (1.4 GHz rest frame) versus γ-ray (integrated above 1 GeV) luminosity plot (left panel). The 1.4 GHz luminosity of PKS 1718−649 was calculated from the ATCA flux, $F_{1.4\ \mathrm{GHz}} = 3.98$ Jy (Maccagni et al. 2014). The source is located in the low radio and γ-ray luminosity region occupied by MAGNs.

The position of PKS 1718−649 in the Γ versus L_γ plot also supports a non-blazar origin of its γ-ray emission: the source occupies the upper left corner, well separated from the blazar sources (Figure 2, right panel). It is interesting to note that its γ-ray luminosity and photon index are similar to those characterizing the giant lobes of Centaurus A (labeled in Figure 2).

Stawarz et al. (2008) proposed a dynamical–radiative model of young radio sources, where the γ-ray emission is produced via IC of circumnuclear (IR-to-UV) photon fields off relativistic electrons in compact, expanding lobes. The level of the non-thermal high-energy emission predicted by the model depends on several source parameters, such as the kinetic jet power, the accretion disk luminosity, and the lobes' compactness: sources with linear sizes <100 pc and jet powers of $\gtrsim 10^{46}$ erg s^{-1} could reach γ-ray luminosities of the order of

[9] For completeness, we added 3C 111 (Grandi et al. 2012), and Cen B (Katsuta et al. 2013), excluded from the clean 3LAC sample because of their low Galactic latitudes, and 3C 120 (Tanaka et al. 2014; Casadio et al. 2015).
[10] FR 0 have radio linear sizes LS $\lesssim$ 10 kpc, radio core powers similar to those of FR Is, and a strong deficit of the corresponding extended radio emission (Baldi et al. 2015).

10^{44} erg s^{-1} or larger (see also Orienti et al. 2011; D'Ammando et al. 2016). The CSO PKS 1718−649 represents an ideal candidate to test this model, due to its linear size of only ∼2 pc and proximity (luminosity distance of 60.4 Mpc). The symmetric radio morphology of PKS 1718−649 suggests that we are observing the source at a large inclination angle, ruling out a γ-ray contribution of the boosted jet emission. The steady flux detected with *Fermi*-LAT is consistent with the γ-ray emission being isotropic and produced in the radio lobes expanding at a sub-relativistic velocity (Giroletti & Polatidis 2009 report a hot spot expansion velocity of $\sim 0.07c$).

A detection in γ-rays may help us establish the nature of the X-ray emission of CSOs (Tengstrand et al. 2009; Siemiginowska et al. 2016). At the angular resolution of the current X-ray observatories, this X-ray emission is usually spatially unresolved and could be a superposition of several distinct components, including that of the disk–corona system and IC emission of the infrared photons of the putative torus off the lobes' electrons (Ostorero et al. 2010). However, a proper test of the above models requires a comparison of the predicted broadband spectral energy distribution with the available multiwavelength data (see Ostorero et al. 2010; Migliori et al. 2012). This is beyond the scope of this Letter and will be discussed in a forthcoming paper.

Is PKS 1718−649 an isolated case or could we expect an increase of the detections of CSOs in γ-rays? So far, γ-ray searches of young radio sources have not provided other significant detections (Migliori et al. 2014; D'Ammando et al. 2016). The 3FGL contains three γ-ray sources tentatively identified as compact steep-spectrum (CSS) radio sources (i.e., sources that likely are more evolved than CSOs): 3C 84 (Kataoka et al. 2010; Dutson et al. 2014), 3C 286, and 4C +39.23B (whose γ-ray association is however doubtful). These are recurrent or restarted radio sources with complex radio morphologies and multiple pairs of lobes on various linear scales. A CSO classification has been proposed for three other γ-ray sources: 4C+55.17 ($z = 0.896$; McConville et al. 2011), PMN J1603−4904 ($z = 0.232$; Müller et al. 2014, 2015; Goldoni et al. 2016), and PKS 1413+135 ($z = 0.247$; Gugliucci et al. 2005). They show the evidence of a CSO-like morphology of the inner radio structures and the absence of the γ-ray and radio variability typically observed in blazars. Differently from PKS 1718−649, all these sources are located at relatively high redshifts and display high γ-ray fluxes with hard spectra. If their γ-ray emission is produced in the lobes and is thus isotropic, the mechanism producing it must be extremely efficient.

Other "γ-ray-emitting CSOs" might be hiding among the large number of unidentified 3FGL γ-ray sources. If this were the case, it would be crucial to define an efficient strategy to unveil them. The example of PKS 1718−649 suggests that a detection in γ-rays is the most feasible for the most compact and nearby CSOs. On the other hand, no detection was reported for another very compact and nearby ($z = 0.076$) CSO, OQ 208 (Orienti et al. 2011; D'Ammando et al. 2016), implying that additional key parameters may play a role. However, given its redshift, OQ 208 would appear a factor of ∼30 fainter than PKS 1718−649, if its intrinsic γ-ray luminosity were the same as that of PKS 1718−649.

We are grateful to the anonymous referee for comments that helped to improve the paper. The authors thank P. Grandi for sharing the data of Figure 2 and J. Ballet, F. D'Ammando, and F. Massaro for useful suggestions. G.M. and S.C. acknowledge the financial support from the UnivEarthS Labex program of Sorbonne Paris Cité (ANR10LABX0023 and ANR11IDEX000502). Ł.S. was supported by Polish NSC grant DEC-2012/04/A/ST9/00083. L.O. acknowledges the grants: INFN InDark, MIUR PRIN2012 "Fisica Astroparticellare Teorica," and "Origin and Detection of Galactic and Extragalactic Cosmic Rays" from UniTo and Compagnia di San Paolo. This research is funded in part by NASA contract NAS8-39073. Partial support was provided by the *Chandra* grants GO4-15099X and GO0-11133X.

REFERENCES

Abdo, A. A., Ackermann, M., Ajello, M., et al. 2010a, ApJ, 720, 912
Abdo, A. A., Ackermann, M., Ajello, M., et al. 2010b, Sci, 328, 725
Acero, F., Ackermann, M., Ajello, M., et al. 2015, ApJS, 218, 23
Ackermann, M., Ajello, M., Albert, A., et al. 2012, ApJS, 203, 4
Ackermann, M., Ajello, M., Atwood, W. B., et al. 2015, ApJ, 810, 14
Atwood, W., Albert, A., Baldini, L., et al. 2013, arXiv:1303.3514
Baldi, R. D., Capetti, A., & Giovannini, G. 2015, arXiv:1510.04272
Buson, S. 2014, ATel, 6067, 1
Casadio, C., Gómez, J. L., Grandi, P., et al. 2015, ApJ, 808, 162
D'Abrusco, R., Massaro, F., Paggi, A., et al. 2014, ApJS, 215, 14
D'Ammando, F., Orienti, M., Giroletti, M. & on behalf of the Fermi Large Area Telescope Collaboration 2016, AN, 337, 59
Dutson, K. L., Edge, A. C., Hinton, J. A., et al. 2014, MNRAS, 442, 2048
Edwards, P. G., Stevens, J., & Ojha, R. 2014, ATel, 6076, 1
Fanaroff, B. L., & Riley, J. M. 1974, MNRAS, 167, 31
Giroletti, M., & Polatidis, A. 2009, AN, 330, 193
Goldoni, P., Pita, S., Boisson, C., et al. 2016, A&A, 586, L2
Grandi, P., Capetti, A., & Baldi, R. D. 2015, arXiv:1512.01242
Grandi, P., Torresi, E., & Stanghellini, C. 2012, ApJ, 751, L3
Gregory, P. C., Vavasour, J. D., Scott, W. K., & Condon, J. J. 1994, ApJS, 90, 173
Gugliucci, N. E., Taylor, G. B., Peck, A. B., & Giroletti, M. 2005, ApJ, 622, 136
Hardcastle, M. J., Cheung, C. C., Feain, I. J., & Stawarz, Ł. 2009, MNRAS, 393, 104
Healey, S. E., Romani, R. W., Taylor, G. B., et al. 2009, yCat, 217, 10061
Huchra, J. P., Macri, L. M., Masters, K. L., et al. 2012, ApJS, 199, 26
Johnston, K. J., Fey, A. L., Zacharias, N., et al. 1995, AJ, 110, 880
Kataoka, J., Stawarz, Ł., Cheung, C. C., et al. 2010, ApJ, 715, 554
Kataoka, J., Stawarz, Ł., Takahashi, Y., et al. 2011, ApJ, 740, 29
Katsuta, J., Tanaka, Y. T., Stawarz, Ł., et al. 2013, A&A, 550, A66
Kino, M., Ito, H., Kawakatu, N., & Nagai, H. 2009, MNRAS, 395, L43
Maccagni, F. M., Morganti, R., Oosterloo, T. A., & Mahony, E. K. 2014, A&A, 571, A67
Massaro, E., Giommi, P., Leto, C., et al. 2009, A&A, 495, 691
Massaro, F., Thompson, D. J., & Ferrara, E. C. 2015, A&ARv, 24, 2
Mattox, J. R., Bertsch, D. L., Chiang, J., et al. 1996, ApJ, 461, 396
Mauch, T., Murphy, T., Buttery, H. J., et al. 2003, MNRAS, 342, 1117
McConville, W., Ostorero, L., Moderski, R., et al. 2011, ApJ, 738, 148
Migliori, G. 2016, AN, 337, 52
Migliori, G., Siemiginowska, A., & Celotti, A. 2012, ApJ, 749, 107
Migliori, G., Siemiginowska, A., Kelly, B. C., et al. 2014, ApJ, 780, 165
Müller, C., Kadler, M., Ojha, R., et al. 2014, A&A, 562, A4
Müller, C., Krauß, F., Dauser, T., et al. 2015, A&A, 574, A117
O'Dea, C. P. 1998, PASP, 110, 493
Ojha, R. 2015, ATel, 7330, 1
Orienti, M. 2016, AN, 337, 9
Orienti, M., Dallasca, D., Giovannini, G., Giroletti, M., & D'Ammando, F. 2011, arXiv:1111.1185
Ostorero, L., Moderski, R., Stawarz, Ł., et al. 2010, ApJ, 715, 1071
Siemiginowska, A., Sobolewska, M., Migliori, G., et al. 2016, ApJ, in press (arXiv:1603.00947)
Skrutskie, M. F., Cutri, R. M., Stiening, R., et al. 2006, AJ, 131, 1163
Stawarz, Ł., Ostorero, L., Begelman, M. C., et al. 2008, ApJ, 680, 911
Tanaka, Y. T., Cutini, S., Ciprini, S., et al. 2014, ATel, 6529, 1
Tengstrand, O., Guainazzi, M., Siemiginowska, A., et al. 2009, A&A, 501, 89
Tingay, S. J., Macquart, J.-P., Collier, J. D., et al. 2015, AJ, 149, 74
Wright, A., & Otrupcek, R. 1990, PKS Catalog (Parkes, Australia: ATNF)